Determination of Strongly Interacting Spin Exchange Paths in $Cu_2(O_3PCH_2PO_3)$ on the Basis of Spin Dimer Analysis

Hyun Woo Bae and Hyun-Joo Koo*

Department of Chemistry and Research Institute of Basic Science of Kyung Hee University, Seoul 130-701, Korea
**E-mail: hjkoo@khu.ac.kr*
Received August 2, 2007

The magnetic properties of the organic/inorganic hybrid copper-methylenediphosphonate, $Cu_2(O_3PCH_2PO_3)$ were examined by performing the spin dimer analysis based on the extended Hückel tight binding method. In $Cu_2(O_3PCH_2PO_3)$ the CuO_3 chains made up of edge-sharing CuO_5 square pyramidal units are inter-linked by O-P-O bridges. The Cu-O-Cu superexchange interactions of the CuO_3 chains are negligibly weak compared with the Cu-O···O-Cu super-superexchange interactions that occur between the CuO_3 chains. The spin exchange interactions of $Cu_2(O_3PCH_2PO_3)$ are dominated by three super-superexchange interactions, which leads to a three-dimensional antiferromagnetic spin lattice. The strongest spin exchange interactions form isolated spin dimers, which suggests that, to a first approximation, the magnetic properties can be described in terms of an isolated spin dimer model.

Key Words : Spin dimer analysis, Superexchange interaction, Super-superexchange interaction, Magnetic orbitals, Electronic structure calculations

Introduction

Organic/inorganic hybrid materials combine the unique characteristics of their components to provide novel solid state structures with composite or new properties. Metal-organophosphonates are a class of such materials with potential applications to catalysis, ion exchange, proton conductivity, photochemistry and intercalation chemistry, and have been studied extensively.[1-3] Copper-methylene-diphosphonate, $Cu_2(O_3PCH_2PO_3)$, prepared by hydrothermal method and structurally characterized,[4] exhibits interesting magnetic properties with broad maximum at approximately 50 K. The magnetic susceptibility in the high temperature region were fitted by the Heisenberg linear antiferromagnetic chain model with g = 2.10, J/k_B = −35.9 K and the Curie-Weiss temperature θ = −55 K. The latter shows the presence of a dominant antiferromagnetic (AFM) coupling. The deviation from the linear chain behavior was observed at low temperatures, which was attributed to the occurrence of a long-range three-dimensional (3D) ordering.[4] To properly interpret the magnetic properties of a given magnetic system, one needs to have a spin lattice model (*i.e.*, the repeat patterns of strongly interacting spin exchange paths) with which to analyze the magnetic data and hence to evaluate the relative strengths of its spin exchange interactions.[5-7] In a magnetic oxide of spin-1/2 Cu^{2+} ions, spin exchange interactions between adjacent ions are either superexchange (SE) involving Cu-O-Cu paths[8] or super-superexchange (SSE) involving Cu-O···O-Cu paths.[5,6] SSE interactions can be much stronger than SE interactions,[5,6,7a] but have frequently been neglected without justifiable reasons. To find a spin lattice model relevant for a magnetic oxide, the relative strengths of both SE and SSE interactions should be evaluated on the basis of proper electronic structure considerations. The spin dimer analysis based on extended Hückel tight binding (EHTB) calculations has been indispensable for deducing spin lattices of magnetic insulators, because it generally reproduces the relative strengths of spin exchange interactions determined from first principles electronic structure calculations.[5,10]

The crystal structure of $Cu_2(O_3PCH_2PO_3)$ consists of highly distorted CuO_5 square pyramid and methylene-diphosphonate units. The CuO_5 units form one-dimensional (1D) CuO_3 chains by sharing their edges, and these CuO_3 chains are cross-linked by the methylenediphosphonates leading to the three dimensional (3D) crystal structure of $Cu_2(O_3PCH_2PO_3)$ (Figure 1)[4] such that the spin exchange interactions can occur through both SE and SSE paths. The

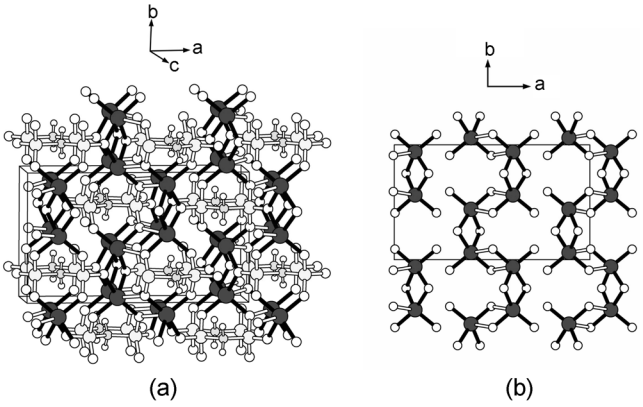

Figure 1. (a) Perspective view of the crystal structure of $Cu_2(O_3PCH_2PO_3)$ and (b) projection view of the edge-sharing CuO_3 chain. The blue, yellow, cyan and large and small white circles represent Cu, P, C, O and H atoms, respectively. The black cylinders indicate the shortest four Cu-O bonds in CuO_5 square pyramidal unit.

observed magnetic susceptibility of $Cu_2(O_3PCH_2PO_3)$ above 50 K has been described in terms of a 1D AFM Heisenberg chain model by considering only the SE interactions of the CuO_3 chains. However, the fitted magnetic susceptibility with this model deviates strongly from the experimental susceptibility below 50 K, and the reason of this poor fit is attributed to the occurrence of a long range magnetic ordering.[4] It has been well established that the spin lattice of a magnetic solid does not necessarily have the same geometrical feature as does the arrangement of its magnetic ions or spin-carrying molecules, because magnetic orbitals are generally anisotropic in shape and because the strength of a spin exchange interaction between adjacent spin sites is determined by the overlap between their magnetic orbitals (*i.e.*, singly occupied molecular orbitals).[5,6,11] In the present work, we examine the spin exchange interactions of $Cu_2(O_3PCH_2PO_3)$ on the basis of EHTB calculations to evaluate its spin exchange interactions and hence identify the spin lattice responsible for its magnetic properties.

Spin Dimer Analysis

The strength of a spin-exchange interaction between two spin sites is described by a spin-exchange parameter $J = J_F + J_{AF}$, where J_F is the ferromagnetic (FM) term ($J_F > 0$) and J_{AF} is the AFM term ($J_{AF} < 0$). In most cases, J_F is very small so that the trends in the J values are well approximated by those in the corresponding J_{AF} values.[5,6] For a spin dimer in which each spin site contains one unpaired spin, the J_{AF} term is approximated by[5]

$$J_{AF} \approx -\frac{(\Delta\varepsilon)^2}{U_{eff}} \quad (1)$$

where U_{eff} is the effective on-site repulsion, which is essentially a constant for a given compound. If the two spin sites are equivalent, $\Delta\varepsilon$ is the energy difference Δe between the two magnetic orbitals representing the spin dimer. When the two spin sites are nonequivalent, $(\Delta\varepsilon)^2 = (\Delta e)^2 - (\Delta e^0)^2$, where Δe^0 is the energy difference between the magnetic orbitals representing each spin site of the spin monomer ($\Delta e^0 = 0$ if the two spin sites are equivalent). In the tight binding approximation, the energy difference $\Delta\varepsilon$ is proportional to the overlap integral, S between the magnetic oribitals. Therefore, the antiferromagnetic term J_{AF} is related to $\Delta\varepsilon$ and S as $J_{AF} \propto -(\Delta\varepsilon)^2 \propto -S^2$.[12,13] In the present work, the Δe and Δe^0 values for various spin dimers are evaluated by performing EHTB calculations.[14,15] For a variety of magnetic solids of transition metal ions, it has been found that their magnetic properties are well described by the $(\Delta\varepsilon)^2$ values obtained from EHTB calculations, when both the d orbitals of the transition-metal ions and s/p orbitals of its surrounding ligands are represented by double-ζ Slater-type orbitals.[16] Our calculations are carried out using the atomic parameters summarized in Table 1.

Table 1. Exponents ζ_i and valence shell ionization potentials H_{ii} of Slater-type orbitals χ_i used for extended Hückel tight-binding calculation[a]

Atom	χ_i	H_{ii} (eV)	ζ_i	C	ζ'_i	C'
Cu	4s	−11.4	2.151	1.0		
Cu	4p	−6.06	1.370	1.0		
Cu	3d	−14.0	7.025	0.4473	3.004	0.6978
P	3s	−18.6	2.367	0.5836	1.499	0.5288
P	3p	−14.0	2.065	0.4908	1.227	0.5940
O	2s	−32.3	2.688	0.7076	1.675	0.3745
O	2p	−14.8	3.694	0.3322	1.659	0.7448
C	2s	−21.4	1.608	1.0000		
C	2p	−11.4	1.568	1.0000		
H	1s	−13.6	1.300	1.0000		

[a] H_{ii}'s are the diagonal matrix elements $\langle\chi_i|H^{eff}|\chi_i\rangle$, where H^{eff} is the effective Hamiltonian. In our calculations of the off-diagonal matrix elements $H_{ij} = \langle\chi_i|H^{eff}|\chi_j\rangle$, the weighted formula was used. See: Ammeter, J.; Bürgi, H.-B.; Thibeault, J.; Hoffmann, R. *J. Am. Chem. Soc.* **1978**, *100*, 3686.

Results and Discussion

Each CuO_5 square pyramidal unit consists of four short and one long Cu-O distances (*i.e.*, 1.934, 1.951, 1.966, 2.054 and 2.255 Å) as shown in Figure 2. It should be noted that the magnetic orbital of a spin monomer CuO_5 is contained in the basal plane of the square pyramid (Figure 2b). In each zigzag CuO_3 chain along the b-axis two adjacent CuO_5 units are connected by sharing their edges such that the Cu···Cu distances of 3.023 and 3.278 Å alternate (Figure 1b). These zigzag chains are linked by PO_3C tetrahedra *via* the O-P-O bridges. Therefore, $Cu_2(O_3PCH_2PO_3)$ has SE interactions in each CuO_3 chain through the edge-sharing dimers as well as SSE interactions between the adjacent CuO_3 chains through the O-P-O bridges. The spin exchange paths of $Cu_2(O_3PCH_2PO_3)$ are shown in Figure 3 and the geometrical parameters associated with them are summarized in Table 2. The SE path J_1 has Cu-O bond distances of 1.966 and 2.054 Å, and unsymmetrical ∠Cu-O-Cu bond angles 100.5 and 94.8°, while the SE path J_2 has unsymmetrical Cu-O bond distance 2.255 and 1.951 Å, and symmetrical ∠Cu-O-Cu bond angles 102.2°. The SSE path J_3 has O···O contact distance of 2.518 Å, which is shorter than the van der Waals distance, but the ∠Cu-O-Cu bond angles are highly unsymmetrical. The SSE path J_4 consists of two O···O contact distances of 2.526 and 2.534 Å, and the ∠Cu-O-Cu bond

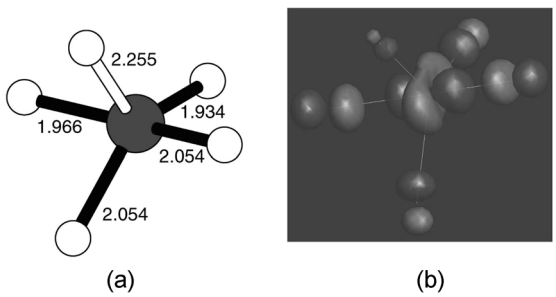

Figure 2. (a) Perspective view and (b) magnetic orbital of a distorted square pyramid CuO_5 in $Cu_2(O_3PCH_2PO_3)$.

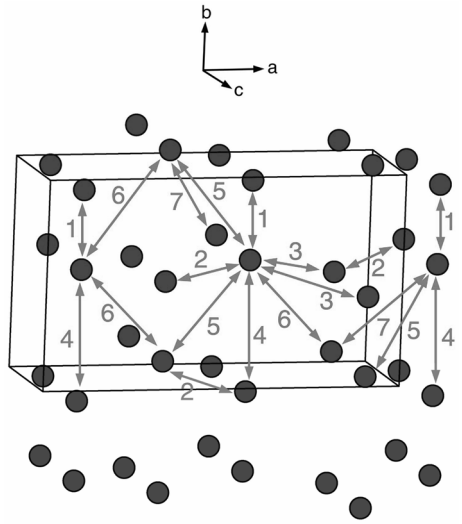

Figure 3. Schematic representation of the spin exchange paths in $Cu_2(O_3PCH_2PO_3)$. The numbers 1 through 7 refer to the spin exchange paths J_1 through J_7, respectively.

Table 2. Geometrical parameters associated with the SE and SSE paths in $Cu_2(O_3PCH_2PO_3)$[a]

(a) SE

Path	Cu···Cu	Cu-O	∠Cu-O-Cu
J_1	3.023	1.966, 1.966	100.5
		2.054, 2.054	94.8
J_2	3.278	2.255, 1.951	102.2
		1.951, 2.255	102.2

(b) SSE

Path	Cu···Cu	O···O	Cu-O	∠Cu-O···O
J_3	4.725	2.518	1.934, 1.966	141.4, 99.4
J_4	4.987	2.526	1.951, 1.951	129.1, 129.1
		2.534	1.934, 1.934	129.3, 129.3
J_5	5.081	2.526	2.255, 1.951	96.3, 129.1
J_6	6.115	2.518	1.966, 1.934	159.5, 141.4
J_7	6.249	2.533	2.054, 1.951	162.4, 142.4

[a]The bond distances are in unit of angstrom and the bond angles are in unit of degree.

angles are highly symmetrical. The O···O contact distance of the SSE path J_5 consists of the long Cu-O bond that does not contain the magnetic orbtials, and the ∠Cu-O-Cu bond angles are unsymmetrical and close to 90º. The O···O contact distance of the SSE path J_6 is slightly shorter than that of the SSE path J_7, but the ∠Cu-O-Cu bond angles of the SSE path J_7 are a little more opened compared with those of the SSE path J_6.

Spin-exchange interactions in magnetic oxides of spin-1/2 Cu^{2+} ions are strongly governed by the arrangement of their CuO_4 square planes containing the magnetic orbitals.[5,6c,7] In the magnetic orbital of a $Cu(O_{eq})_4$ square plane (the oxygen atoms forming the CuO_4 square plane are referred to as O_{eq}), the Cu $3d_{x^2-y^2}$ orbital makes σ antibonding with the 2p orbitals of the four O_{eq} atoms. A crucial factor determining

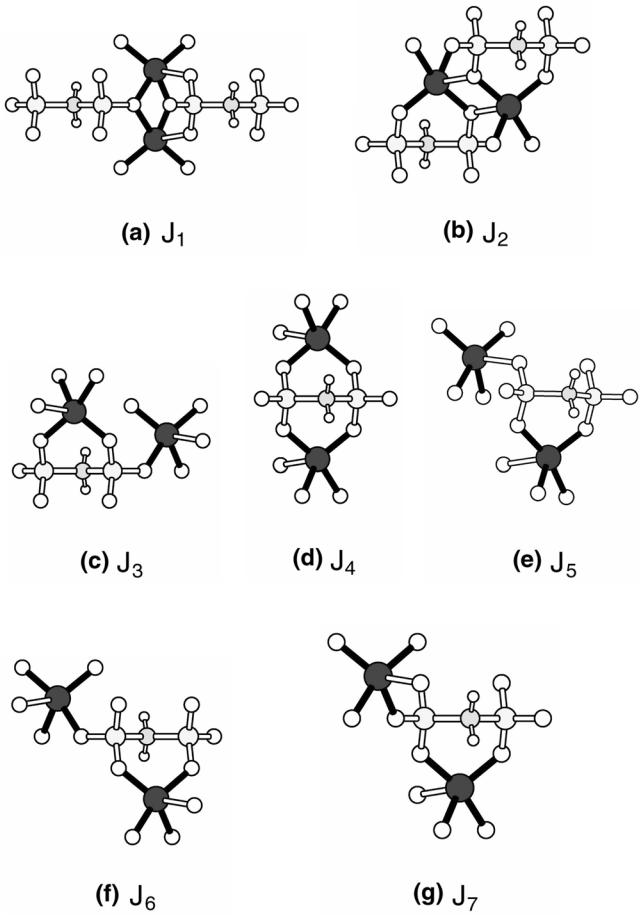

Figure 4. Spin dimers associated with the spin exchange paths J_1 through J_7 in $Cu_2(O_3PCH_2PO_3)$.

the strength of a spin-exchange interaction between Cu^{2+} ions is not the Cu $3d_{x^2-y^2}$ orbitals but the O 2p orbitals of their magnetic orbitals (*i.e.*, the "tails of the magnetic orbitals) because the spin exchange between two adjacent Cu^{2+} ions depends on the overlap between their magnetic orbitals, which is, in turn, determined by the overlap between their tails.[5,6c,6e,7] Therefore, from the viewpoint of the magnetic orbital, one might expect that the spin exchange interactions through the SSE paths J_4, J_6 and J_7 are stronger than those J_3 and J_5, since the overlap increases as both ∠Cu-O···O bond angles become larger and as the O···O distance becomes shorter and lies within the van der Waals distance and the strength of the SSE interaction is proportional to the overlap S.[5,6,12,13] However, it is hard to predict the relative strengths of spin exchange interactions between the SE and SSE paths without electronic structure calculations.

Results of spin dimer analyses for the spin dimers shown in Figure 4 are summarized in Table 3, which shows that the SSE interactions J_4, J_6 and J_7 are stronger than the SSE interactions J_3 and J_5, while the SE interactions J_1 and J_2 are negligibly weak. The strongest spin exchange interactions J_4 form isolated spin dimers (Figure 5a), and these dimers interact through the second strongest spin exchange interactions J_6 (with J_6/J_4 = 0.53) to form the corrugated two-

Table 3. Values of $(\Delta\varepsilon)^2$ calculated for the SE and SSE interactions of $Cu_2(O_3PCH_2PO_3)$

Path	$(\Delta\varepsilon)^{2\ a,b}$	Relative value
J_1	630	0.02
J_2	60	0.00
J_3	890	0.03
J_4	27960	1.00
J_5	2600	0.09
J_6	14860	0.53
J_7	8030	0.29

[a]The values of $(\Delta\varepsilon)^2$ are in units of $(meV)^2$. [b]$\Delta e^0 = 0$ because the two spin sites are equivalent.

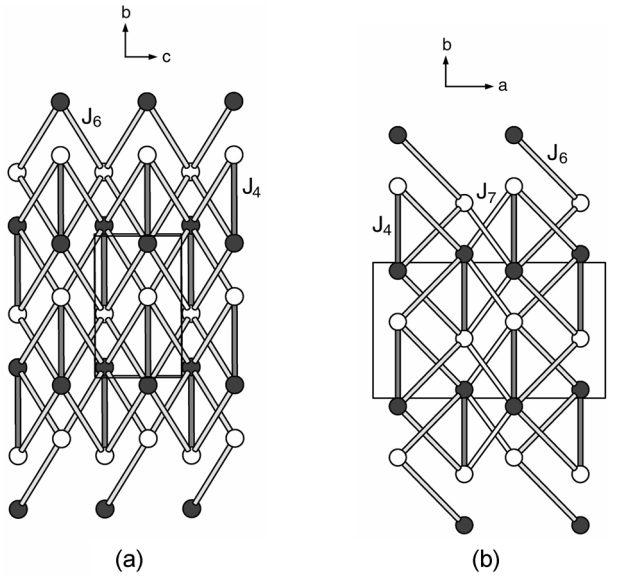

Figure 5. Schematic representation of the AFM spin lattices expected for $Cu_2(O_3PCH_2PO_3)$. (a) 2D AFM lattice made up of J_4 and J_6, and (b) 3D AFM lattice made up of the 2D AFM lattices connected by J_7. The red, cyan and yellow cylinders represent the paths J_4, J_6 and J_7, respectively, and the gray and white circles indicate spin up and down spin states of Cu^{2+} ion sites, respectively.

dimensional (2D) AFM spin lattice in which each spin site to four adjacent spin sites connected by J_6. These 2D AFM lattices are connected by the third strongest spin exchange interactions J_7 (with $J_7/J_4 = 0.29$) to form the 3D AFM spin lattice (Figure 5b). All other spin exchange interactions are negligible. For the SSE interactions between two spin sites *i* and *j*, we also calculated the overlap integrals S_{ij} between the magnetic orbitals. Note that the magnetic orbital of a spin site is the singly occupied molecular orbital of the spin monomer representing the spin site. In general, the $(\Delta\varepsilon)^2$ values are proportional to the $(S_{ij})^2$ values, which are listed in Table 4. The $(S_{ij})^2$ values of the SSE paths J_4, J_6 and J_7 are stronger than the SSE path J_3 and J_5, which is consistent with the result of the spin dimer analyses. The trend in the relative strengths of overlap integrals can be understood by considering the nature of the magnetic orbital (Figure 2b) and the SSE paths (Figure 4). For the SSE path J_4, the p-orbital tails of the magnetic orbitals have a σ-type overlap

Table 4. Values of S_{ij}^2 calculated for the SSE interactions of $Cu_2(O_3PCH_2PO_3)$

Path	$S_{ij}^2 \times 10^6$	Relative value
J_3	4	0.08
J_4	49	1.00
J_5	0.3	0.00
J_6	25	0.51
J_7	16	0.33

through the O···O contacts. For the SSE path J_5, however, there is no overlap between the magnetic orbitals. Thus, the overlap integral of the SSE path J_4 is much stronger than that of the path J_5. For the paths J_6 and J_7, there is only one O···O contact between the magnetic orbitals, so their overlap integrals are weaker than that of the path J_4. Thus, our spin dimer analysis suggests that, to a first approximation, the magnetic properties can be described in terms of an isolated spin dimer by considering only the strongest spin exchange interaction. This explains the occurrence of a broad maximum (around 50 K) in the magnetic susceptibility of $Cu_2(O_3PCH_2PO_3)$, and also suggests that $Cu_2(O_3PCH_2PO_3)$ should exhibit a spin gapped character.[7b,17] The latter view is consistent with the fact that the magnetic susceptibility decreases rapidly with decreasing temperature below 50 K.[4] The observed magnetic susceptibility does not show a spin gap, but this might be due to the presence of a minute amount of magnetic impurities.

Concluding Remarks

In $Cu_2(O_3PCH_2PO_3)$ the CuO_3 chains made up of edge-sharing CuO_5 square pyramidal units are inter-linked by O-P-O bridges. The present work shows that the SE interactions of the CuO_3 chains are negligibly weak compared with the SSE interactions that occur between the CuO_3 chains. The spin exchange interactions of $Cu_2(O_3PCH_2PO_3)$ are dominated by three SSE interactions J_4, J_6 and J_7, which leads to a 3D AFM spin lattice. The strongest spin exchange interactions J_4 form isolated spin dimers (Figure 5a), which suggests that, to a first approximation, the magnetic properties can be described in terms of an isolated spin dimer. This in turn suggests that $Cu_2(O_3PCH_2PO_3)$ might be a spin gapped system. Further experimental studies are necessary to verify this prediction.

Acknowledgments. H.-J. K. is gratefully acknowledging the support by Defense Acquisition Program Administration and Agency for Defence Development, and thanks Professor M.-H. Whangbo (North Carolina State University, Raleigh) for invaluable discussion. H.-W.B was supported by the second stage of the Brain Korea 21 program in Korea.

References

1. Wang, J. D.; Clearfield, A.; Peng, G.-Z. *Mater. Chem. Phys.* **1993**, *35*, 208.

2. Stein, E.; Clearfield, A.; Subramanian, M. A. *Solid State Ion* **1996**, *83*, 113.
3. Vermeulen, L. A.; Snover, J. L.; Sapochak, L. S.; Thompson, M. E. *J. Am. Chem. Soc.* **1993**, *115*, 11767.
4. Burkholder, E.; Golub, V. O.; O'Connor, C. J.; Zubieta, J. *Inorg. Chim. Acta* **2002**, *340*, 127.
5. For reviews see: (a) Whangbo, M.-H.; Koo, H.-J.; Dai, D. *J. Solid State Chem.* **2003**, *176*, 417. (b) Whangbo, M.-H.; Dai, D.; Koo, H.-J. *Solid State Sci.* **2005**, *7*, 827.
6. (a) Koo, H.-J.; Whangbo, M.-H. *Inorg. Chem.* **2001**, *40*, 2169. (b) Koo, H.-J.; Whangbo, M.-H.; VerNooy, P. D.; Torardi, C. C.; Marshall, W. J. *Inorg. Chem.* **2002**, *41*, 4664. (c) Whangbo, M.-H.; Koo, H.-J.; Dai, D.; Jung, D. *Inorg. Chem.* **2003**, *42*, 3898. (d) Koo, H.-J.; Whangbo, M.-H.; Lee, K.-S. *Inorg. Chem.* **2003**, *42*, 5932. (e) Koo, H.-J.; Dai, D.; Whangbo, M.-H. *Inorg. Chem.* **2005**, *44*, 4359.
7. (a) Belik, A. A.; Azuma, M.; Matsuo, A.; Whangbo, M.-H.; Koo, H.-J.; Kikuchi, J.; Kaji, T.; Okubo, S.; Ohta, H.; Kindo, K.; Takano, M. *Inorg. Chem.* **2005**, *44*, 6632. (b) Koo, H.-J.; Whangbo, M.-H. *Inorg. Chem.* **2006**, *45*, 4440. (c) Koo, H.-J.; Lee, C.; Wilson-Short, G. B.; Dai, D.; Whangbo, M.-H. *Inorg. Chem.* **2007**, *46*, 2498.
8. Goodenough, J. B. *Magnetism and the Chemical Bond*; Wiley: Cambridge, MA, 1963.
9. Dai, D.; Whangbo, M.-H.; Koo, H.-J.; Rocquefelte, X.; Jobic, S.; Villesuzanne, A. *Inorg. Chem.* **2005**, *44*, 2407.
10. (a) Whangbo, M.-H.; Koo, H.-J.; Lee, K.-S. *Solid State Commun.* **2000**, *114*, 77. (b) Koo, H.-J.; Whangbo, M.-H. *J. Solid State Chem.* **2000**, *151*, 96.
11. Koo, H.-J.; Lee, K.-S.; Whangbo, M.-H. *Inorg. Chem.* **2006**, *45*, 10743.
12. Kahn, O. *Molecular Magnetism*; VCH Publisher: Weinheim, 1993.
13. Hay, P. J.; Thibeault, J. C.; Hoffmann, R. *J. Am. Chem. Soc.* **1975**, *97*, 4884.
14. Hoffmann, R. *J. Chem. Phys.* **1963**, *39*, 1397.
15. Our calculations were carried out by employing the CAESAR 2.0 (Crystal and Electronic Structure Analyzer) program package. (This program can be downloaded free of charge from the website, http://chvamw.chem.ncsu.edu/).
16. Clementi, E.; Roetti, C. *Atomic Data Nuclear Data Tables* **1974**, *14*, 177.
17. (a) Bleaney, B.; Bowers, K. D. *Proc. R. Soc. London, Ser. A* **1952**, *214*, 451. (b) Ueda, Y. *Chem. Mater.* **1998**, *10*, 2653. (c) Johnston, D. C.; Kremer, R. K.; Troyer, M.; Wang, X.; Klümper, A.; Bud'ko, S. L.; Panchula, A. F.; Canfield, P. C. *Phys. Rev. B* **2000**, *61*, 9558. (d) Vasil'ev, A. N.; Markina, M. M.; Popova, E. A. *Low Temp. Phys.* **2005**, *31*, 203. (e) Nakajima, T.; Mitamura, H.; Ueda, Y. *J. Phys. Soc. Jpn* **2006**, *75*, 54706.